

# Design of Intelligent Financial Data Management System Based on Higher-Order Hybrid Clustering Algorithm

Haitao Lu <sup>Corresp. 1</sup>

<sup>1</sup> Department of Accounting, Henan Institute of Economics and Trade, Zhengzhou, China

Corresponding Author: Haitao Lu  
Email address: lu001710@163.com

Amid the ever-expanding landscape of financial data, the importance of predicting potential risks through artificial intelligence methodologies has steadily risen. To achieve prudent financial data management, this manuscript delves into the domain of intelligent financial risk forecasting within the scope of system design. It presents a data model based on the variational encoder (VAE) enhanced with an attention mechanism, meticulously tailored for forecasting a company's financial peril. The framework embarks on its journey by encoding and enhancing multidimensional data through VAE. It then employs the attention mechanism to enrich the outputs of the VAE network, thereby demonstrating the apex of the model's clustering capabilities. In the experimentation, we subject the model to a battery of training tests using diverse datasets. The results conspicuously highlight the model's commendable performance in comparison to publicly available datasets, surpassing numerous deep clustering networks at this juncture. In the realm of financial data, the ATT-VAE model, as presented within this treatise, achieves a clustering accuracy index exceeding 0.7, a feat demonstrably superior to its counterparts in the realm of deep clustering networks. The method outlined herein provides algorithmic foundations and serves as a pivotal reference for the prospective domain of intelligent financial data governance and scrutiny.

# Design of Intelligent Financial Data Management System Based on Higher-Order Hybrid Clustering Algorithm

1

2 Haitao Lu\*

3

4 Department of Accounting, Henan Institute of Economics and Trade, Zhengdong New District  
5 450018, Zhengzhou, Henan, China.

6

7 Corresponding Author:

8 Haitao Lu

9 No.58, Hubei Road, Longzi University Park, Longzi Lake, Zhengzhou

10 Email address: lu001710@163.com

11

## 12 Abstract

13 Amid the ever-expanding landscape of financial data, the importance of predicting potential  
14 risks through artificial intelligence methodologies has steadily risen. To achieve prudent financial  
15 data management, this manuscript delves into the domain of intelligent financial risk forecasting  
16 within the scope of system design. It presents a data model based on the variational encoder  
17 (VAE) enhanced with an attention mechanism, meticulously tailored for forecasting a company's  
18 financial peril. The framework embarks on its journey by encoding and enhancing  
19 multidimensional data through VAE. It then employs the attention mechanism to enrich the  
20 outputs of the VAE network, thereby demonstrating the apex of the model's clustering capabilities.  
21 In the experimentation, we subject the model to a battery of training tests using diverse datasets.  
22 The results conspicuously highlight the model's commendable performance in comparison to  
23 publicly available datasets, surpassing numerous deep clustering networks at this juncture. In the  
24 realm of financial data, the ATT-VAE model, as presented within this treatise, achieves a  
25 clustering accuracy index exceeding 0.7, a feat demonstrably superior to its counterparts in the  
26 realm of deep clustering networks. The method outlined herein provides algorithmic foundations  
27 and serves as a pivotal reference for the prospective domain of intelligent financial data  
28 governance and scrutiny.

29 **Keywords:** CNN; VAE; Attention Mechanism; deep clustering; Finance risk prediction.

## 30 1 Introduction

31

32 With the continuous development of the global economy, refined quantitative analysis of  
33 finance has become an indispensable part of decision-making for enterprises and investors.  
34 Financial analysis can help investors and clients evaluate the financial health of a company,  
35 thereby completing corresponding tasks from a more scientific perspective. Traditional financial  
36 analysis methods include financial ratios, financial statement analysis, trend analysis, and  
37 comparative analysis. In the study of financial information, the focus needs to monitor the financial  
38 risks of companies. Once financial risks occur, especially for listed companies, it will bring huge  
39 losses or even bankruptcy to the enterprise. Financial risks may also lead to deterioration of the  
40 company's operating conditions, decline in stock prices, loss of investor confidence, and other  
41 issues, thereby affecting the long-term development and interests of the company. Therefore,  
42 monitoring the financial condition of a company and evaluating its financial health through more  
43 intelligent means has become a research focus in the current financial and financial data  
44 management fields. [2].

45 The types of financial data are complex, especially for large listed companies, which have a  
46 massive amount of financial data, such as the company's profits, cash flow, liabilities, and revenue  
47 on the same day. In addition to these numerical types of data, it usually includes text and chart  
48 forms of data. Therefore, leveraging the data processing advantages of machine learning and  
49 deep learning methods to achieve multimodal data fusion is very important for intelligent  
50 management of financial data. The task of financial analysis is to identify financial risks through  
51 the clustering method of multimodal data, which is a clustering problem. Traditional machine  
52 learning methods typically rely on manually designed features and have limited ability to handle  
53 massive amounts of data. Some traditional clustering algorithms, such as K-means clustering,  
54 are very sensitive to the selection of initial cluster centers. Different initial values may lead to  
55 different clustering results, and it is necessary to run the algorithm multiple times to obtain stable  
56 results. If financial analysis involves textual data, traditional machine learning methods may not  
57 be as flexible in processing and analyzing textual features as deep learning methods.

58 Deep learning models are usually more suitable for situations with complex data modalities  
59 and diverse properties, such as auto-encoder. Autoencoder is an unsupervised learning model  
60 commonly used for feature learning and data dimensionality reduction [4]. Deep models such as  
61 CNN, LSTM, and other modeling methods that excel in processing time series data [5] can capture  
62 implicit features in time series, thereby completing tasks such as data classification, regression,  
63 and prediction. These methods are used in fields such as stock prediction and futures analysis in  
64 the financial field. For the design of an intelligent financial system data system, in addition to  
65 ensuring basic data storage and visualization functions, it also requires a certain level of intelligent  
66 decision-making ability. Using deep learning methods to identify financial risks based on  
67 multimodal data is crucial for the construction of financial systems. This article proposes a  
68 clustering model based on deep networks for intelligent management of financial data, aiming to  
69 achieve intelligent clustering of financial data risks. The specific contributions are as follows::

70 (1) Synergizing Multiple Techniques: Our method amalgamates the Variational  
71 Autoencoder (VAE) and the attention mechanism, facilitating multi-dimensional data

72 clustering and enhancing financial data analysis. The combination of these techniques  
73 maximizes the performance of each method and improves data clustering capabilities.  
74 (2) Holistic Financial Data Analysis: Our approach not only enables high-quality clustering  
75 analysis of financial data but also supports intelligent financial system management,  
76 substantially reducing human intervention for sustainable development.  
77 (3) Model Validation: We validate our approach against established clustering databases  
78 and benchmark it against common deep clustering network methods. The experimental  
79 results demonstrate the superior performance of the proposed ATT-VAE method in  
80 analyzing financial risk data.

81 The subsequent sections of this paper are organized as follows: Section 2 presents related  
82 work, while Section 3 introduces the proposed methods, VAE, and the Attention mechanism.  
83 Section 4 provides details about the experiments, and Section 5 offers conclusions..

## 84 **2 Related works**

### 85 2.1 Intelligent management of financial data

86 The realm of financial risk early warning holds a pivotal standing within the purview of  
87 financial management and investment decision-making. As the sands of time have drifted by, the  
88 focus of inquiry and the arsenal of analytical tools have undergone a progressive evolution. It has  
89 transitioned from the examination of a scant number of company samples in its nascent stages  
90 to the comprehensive scrutiny of a multitude of companies replete with complete datasets.  
91 Concurrently, the means of analysis has advanced from the rudimentary utilization of financial  
92 indicator ratios to the construction of secondary indicators. It has further embraced the infusion of  
93 mathematical and statistical methodologies to give rise to multivariate discriminant analysis  
94 models, epitomized by the Z models. Presently, the landscape resonates with the widespread  
95 adoption of diverse machine learning and deep learning models <sup>[6]</sup>. Ohlson's seminal work,  
96 expounded in <sup>[7]</sup>, unveiled a Logistic-based early warning model. This model, distilled through the  
97 meticulous examination of over 2,000 solvent and insolvent companies, aspires to prognosticate  
98 the probability distribution of corporate bankruptcy. Shin and colleagues <sup>[8]</sup> embarked on a  
99 pioneering exploration into the application of support vector machine models within the sphere of  
100 machine learning for financial risk prognosis. Empirical evidence underscored the supremacy of  
101 the SVM model over traditional multivariate discriminant analysis and Logit models in the realm  
102 of financial risk assessment. With the burgeoning computational prowess, the mantle was passed  
103 to neural network models and CNN models, both of which garnered resounding success within  
104 this domain <sup>[9]</sup>. Odom et al <sup>[10]</sup> championed a financial risk early warning model leveraging artificial  
105 neural networks. They painstakingly assembled a dataset teeming with an equitable number of  
106 precarious and stable companies for in-depth analysis, ultimately yielding commendable  
107 predictive outcomes. Marcano et al ventured into the realm of meta plasticity neural networks  
108 (AMMLP) and engineered an enhanced ANN model for credit default risk evaluation <sup>[11]</sup>.

109 Furthermore, Hosaka introduced a novel approach, transmuting the financial indicators of  
110 insolvent companies into grayscale images. Subsequently, they harnessed a CNN deep learning  
111 model to prognosticate corporate bankruptcy risks with promising outcomes <sup>[12]</sup>.

112

## 113 2.2 Research on Traditional Clustering Methods

114 Traditional clustering algorithms, often referred to as early clustering algorithms, exhibit  
115 commendable performance on small-scale, low-dimensional datasets. Their development has  
116 reached a mature stage, owing to their intuitively comprehensible principles and straightforward  
117 implementation. These methods find extensive utility across various domains, particularly in the  
118 realm of image processing. Prominent among these traditional clustering algorithms are the K-  
119 Means algorithm and the spectral clustering algorithm, among others. Typically, these algorithms  
120 take as input a data matrix composed of image or text features, employing diverse clustering  
121 strategies to gauge the similarity relationships among these features and subsequently generating  
122 clustering outcomes <sup>[13]</sup>. The K-Means clustering algorithm halts when it attains a local optimum  
123 solution. Notably, it is tailored for numerical data clustering. It boasts the virtues of simplicity and  
124 efficiency, characterized by low algorithmic complexity. However, it bears certain drawbacks, such  
125 as sensitivity to predetermined values for the number of clusters, vulnerability to noise and  
126 outliers, and suboptimal performance on datasets with non-spherical clusters. In an endeavor to  
127 enhance the K-Means algorithm's performance, the DIANA split hierarchical clustering algorithm  
128 was introduced, treating the provided data as a cluster structure and progressively partitioning  
129 the most recently formed cluster into smaller clusters based on cluster diameter or average  
130 dissimilarity <sup>[14]</sup>.

131 Guha et al. introduced the CURE algorithm, an improved hierarchical clustering method that  
132 leverages a representative subset of points to depict a cluster, departing from the conventional  
133 approach of using all points or a single center of mass. This modification renders it more resilient  
134 to isolated points and equips it to identify clusters characterized by complex shapes and varying  
135 sizes <sup>[15]</sup>. The incorporation of fuzzy set theory into hard clustering algorithms, assigning each  
136 sample a certain probability of belonging to a particular class, has birthed fuzzy clustering  
137 algorithms <sup>[16]</sup>. Krinidis et al. contributed a robust C-mean clustering algorithm for fuzzy local  
138 information, introducing a fuzzy local neighborhood factor to amalgamate local spatial and  
139 grayscale information, thereby diminishing the clustering method's sensitivity to noise <sup>[17]</sup>.

140 Karlekar et al. introduced a fuzzy clustering technique employing nonlinear distances, substituting  
141 s-distance for the Euclidean distance metric, resulting in more robust natural clustering outcomes  
142 <sup>[18]</sup>. Beyond K-Means approaches, spectral clustering and its derivatives have garnered significant  
143 traction in contemporary clustering methodologies. Wang et al. introduced constrained spectral  
144 clustering, augmenting spectral clustering with additional sub-information to bolster clustering

145 results. By leveraging pairwise constraints, this approach tackles challenging segmentation tasks  
146 by determining whether two points are linked based on the introduced edge information [19]. Chen  
147 et al. proposed a parallel spectral clustering approach for deployment in distributed systems [20].  
148 They juxtaposed two methods for approximating dense matrices to address concerns related to  
149 memory consumption and computational time scalability in spectral clustering. Ultimately, they  
150 opted to retain the nearest neighbors to sparsify the matrix, a strategy applicable to solving  
151 problems within distributed systems. Traditional clustering methodologies can also harness  
152 representation learning techniques for feature extraction, including subspace representation  
153 learning and deep network representation learning. This circumvents the limitations of  
154 conventional methods when confronted with high-dimensional data.

155

### 156 2.3 Research on clustering algorithms based on deep learning

157 Deep learning based clustering methods are categorized into generative model based  
158 methods and discriminative model based methods based on the nature of the network model and  
159 the results of these two types of methods can be subdivided again as shown in Figure 1:

160

161

Figure 1 The deep clustering methods

162 Deep clustering methods encompass a diverse array of techniques, including those  
163 predicated on VAE, GAN, intricate deep models, and GNN. The architecture of autoencoder-  
164 based clustering methods typically comprises two fundamental components: the autoencoder  
165 module and the similarity measure module [21]. Various methods adopt distinct training strategies,  
166 with one of the pioneering approaches being the inception of deep embedding clustering [22]. This  
167 method disentangles the dimensionality reduction process from the similarity metric computation  
168 within the framework. It commences with the acquisition of a proficient encoder model via self-  
169 encoder training, subsequently proceeding to joint training of the encoder and similarity metric  
170 modules. However, this approach renders the embedded features overly reliant on the initialized  
171 encoder model, which can exert an impact on clustering outcomes. Building upon this foundation,  
172 a fusion between the traditional K-means method and deep clustering methodology was realized,  
173 culminating in the co-optimization of dimensionality reduction and similarity metrics, thereby  
174 yielding more optimized results [23]. Presently, deep learning-based clustering methodologies  
175 predominantly hinge on similarity metrics. In pursuit of neighborhood relationships, these methods  
176 typically employ local constraints during the similarity metric computation process. While local  
177 constraints effectively ascertain the similarity of points within clusters, they may falter in precisely  
178 distinguishing the class attributes of points positioned at the cluster periphery. Consequently, this  
179 can result in indistinct cluster boundaries within the feature space [24]. Moreover, approaches  
180 grounded in self-coder models can also be amalgamated with spectral clustering, subspace  
181 clustering, and other techniques. The choice of neural networks for encoding can significantly  
182 impact outcomes, with convolutional neural networks often outperforming fully connected neural  
183 networks [25-26].

184 The evolution of segment clustering research clearly demonstrates that contemporary deep  
 185 learning methods offer superior practical utility when juxtaposed with traditional clustering  
 186 approaches. Furthermore, the amalgamation of VAE with CNN and other techniques augments  
 187 the robustness of self-supervised and semi-supervised models. Given the sheer volume of  
 188 financial data, along with the challenges of missing data and the impracticality of manual labeling,  
 189 the adoption of advanced deep clustering methods assumes paramount significance in the  
 190 domain of financial system management. Consequently, this manuscript proffers a novel  
 191 proposition: the enhancement of unsupervised analysis of financial data through the synergistic  
 192 integration of VAE and existing CNN methodologies.

### 193 3 Methodology

194 CNN is an influential deep learning model extensively deployed in computer vision tasks,  
 195 encompassing image classification, target detection, and image segmentation. The watershed  
 196 moment for CNNs occurred in 2012 with the advent of the AlexNet network [27], which solidified  
 197 the standing of convolutional neural networks in the domain of deep learning. In this study, we  
 198 opt to employ AlexNet for data analysis. In addition to the convolution operation outlined in  
 199 equation (1), AlexNet augments network generalization performance by incorporating local  
 200 normalization (LRN). The LRN is computed as depicted in equation (2):

$$201 \quad (I * K)(x, y) = \sum_{i=-a}^a \sum_{j=-b}^b I(x+i, y+j) \cdot K(i, j) \quad (1)$$

$$202 \quad R(x, y, k) = \frac{A(x, y, k)}{\left( \kappa + \alpha \sum_{i=\max(0, k-\frac{n}{2})}^{\min(N-1, k+\frac{n}{2})} (A(x, y, i))^2 \right)^{\beta}} \quad (2)$$

203  
 204 In equation (1), I represents the input data, K is the convolution kernel, i, j are the coordinates  
 205 of the convolution kernel, and a and b are the radii of the convolution kernel. For Alexnet's special  
 206 link LRN, R in Eq. (2) represents the output response, A is the original unnormalized response,  
 207 and the rest of the adjustable parameters are used to control the degree of normalization and  
 208 parameters such as the window and the number of channels. In addition to this, models such as  
 209 ResNet, GoogleNet, etc. are widely used methods in CNN-like networks [28]. The clustering ability  
 210 of the model can be greatly enhanced by augmenting the current information through  
 211 convolutional neural networks.

212

#### 213 3.2 Self-Encoder (AE) Models and Variational Self-Encoders (VAE)

214 AE and VAE both belong to the realm of unsupervised learning models that find prominent  
 215 utility in deep learning for uncovering latent data representations. They serve a multitude of

216 purposes, including feature extraction, data compression, and dimensionality reduction. AE  
217 constitutes a neural network architecture comprising two principal components: an encoder and  
218 a decoder. The encoder serves to map input data into a lower-dimensional representation, while  
219 the decoder endeavors to reconstruct this lower-dimensional representation back into the original  
220 input data. The primary objective of AE is twofold: to achieve accurate reconstruction of the input  
221 data and to distill essential features of the input data within the low-dimensional representation  
222 generated by the encoder. This is illustrated in Figure 2:

223

224

Figure 2 Structure of self-encoder

225 For encoding and decoding of the encoder is done through function mapping, after  
226 completion, the model training needs to be realized through the definition of the loss function and  
227 objective function, which are defined as shown in equations (3) and (4):

228

$$L(x, x') = \frac{1}{n} \sum_{i=1}^n (x_i - x'_i)^2 \quad (3)$$

229 Where:  $L(x, x')$  denotes the loss function, representing the original input  $x$  and reconstructed input  
230  $x'$  mean square error between the original and reconstructed inputs.

231 The goal of this loss function is to minimize the difference between the reconstructed data  
232 and the original input, allowing the AE to learn a valid representation of the data. However,  
233 depending on the specific task and data type, other loss functions can be chosen, such as the  
234 cross-hashing loss. The objective function is then expressed by equation (4).

235

$$\theta^* = \arg \min_{\theta} \frac{1}{N} \sum_{i=1}^N L(x^{(i)}, x'^{(i)}) \quad (4)$$

236 Where:  $\theta^*$  denotes the model parameters to be optimized to minimize the loss function.  $N$   
237 denotes the number of samples in the training dataset.  $L(x^{(i)}, x'^{(i)})$  denotes the loss function that  
238 measures the number of samples in the first  $i$  original input of the first training sample  $x^{(i)}$  and  
239 reconstructed input  $x'^{(i)}$  between the original and reconstructed inputs of the first training sample,  
240 and the mean square error or other loss measures. The optimal output of the model can be  
241 obtained by optimizing the objective function and the loss function.

242

### 243 3.3 Overall framework of the attention-based VAE

244 VAE has the following advantages over ordinary AE: a VAE is a generative model that learns  
245 valid data representations and generates new samples; its latent space is continuous and  
246 interpretable, allowing operations such as interpolation, sampling, and so on, to generate diverse  
247 samples; the latent representations are more easily interpretable, which helps with a variety of  
248 downstream tasks; and the generated samples are typically of higher quality because the VAE  
249 generates samples by learning the latent distributions, rather than just replicating the training data  
250 points. The structure of the VAE is shown in Figure 3:

251

252

Figure 3 The framework for the VAE

253

254 Figure 3 underscores the key distinction between VAE and AE. In VAE, an additional  
 255 statistical module comes into play, which corresponds to the encoder component of the VAE,  
 256 while the generator aligns with the decoder, symmetrically positioned with respect to the encoder.  
 257 The encoder undertakes the computation of mean and variance for each input, assigning a normal  
 258 distribution to each input data point. It's essential to ensure that the variance in this normal  
 259 distribution is not zero, as a zero variance would lead to a loss of randomness, making it  
 260 challenging for the decoder to effectively reconstruct the samples in the presence of noise. During  
 261 the sampling process, as sampling itself is a non-differentiable operation, the sampled result is  
 262 not directly amenable to gradient-based optimization. To circumvent this issue, the re-  
 263 parameterization technique is employed, allowing for the design of a differentiable sampling  
 264 operation. This enables the optimization of the mean-variance model in reverse. The probability  
 265 distribution of the encoder is encapsulated in equation (5).

266

$$q_{\theta}(z|x) = \mathcal{N}(\mu_{\theta}(x), \sigma_{\theta}(x)^2) \quad (5)$$

267 where  $\theta$  denotes the parameters of the encoder, and  $\mu_{\theta}(x)$  and  $\sigma_{\theta}(x)$  denote the mean and  
 268 standard deviation, respectively. Latent space sampling.

269

$$z = \mu_{\theta}(x) + \sigma_{\theta}(x) \cdot \epsilon \quad (6)$$

270 where  $\epsilon$  is the random noise sampled from the standard normal distribution. The normal  
 271 distribution feature is also introduced in the decoder section with the conditions shown in equation  
 272 (7):

273

$$p_{\phi}(x|z) \quad (7)$$

274 This means that given the potential variables  $z$  that generates the data in the case of  $x$  of the  
 275 conditional distribution. The parameters of the decoder are denoted by  $\phi$ .

276 In this paper, in order to enhance the model performance, we add Attention Mechanism,  
 277 which is a technique widely used in deep learning to enhance the neural network's attention to  
 278 certain parts of the input data, thus improving the model performance. In Attention Mechanism,  
 279 there are usually three key components, Query, Key and Value features and the model  
 280 enhancement is achieved by Attention Score, Attention Weight and Weighted Sum,  $Q$  denotes  
 281 the query and  $K$  denotes the key, then the Attention Score can be expressed as (8)-(10):

282

$$\text{Attention}(Q,K) = \frac{Q \cdot K}{\sqrt{d_k}} \quad (8)$$

283

$$\text{Attention\_Weights}(Q,K) = \text{softmax}(\text{Attention}(Q,K)) \quad (9)$$

284

$$\text{Attention\_Output}(Q,K,V) = \sum_i \text{Attention\_Weights}(Q,K)_i \cdot V_i \quad (10)$$

285

where  $d_k$  denotes the dimension of the key. The core idea of the attention mechanism is to

286 assign the weights of the values based on the relationship between the query and the keys in  
287 order to better capture the relevant information of the input data in different tasks and different  
288 contexts. This dynamic attention mechanism enables the neural network to better handle  
289 sequential data and improves generalization ability of the model. The model based on the  
290 attention mechanism established in this paper is shown in Figure 4:

291

292

Figure 4 Framework of the proposed ATT-VAE

293 In Figure 4, after completing the data input, we realized the feature extraction enhancement of  
294 the data by VAE, and completed the final model optimization by using the attention mechanism  
295 on the right side to realize the clustering judgment of the system.

## 296 4 Experiment setup and Result analysis

### 297 4.1 Datasets

298 Considering the characteristics of the clustering method and the characteristics of the data  
299 used, the data used in this paper include the following five:

300 AwA (<https://cvml.ist.ac.at/AwA/>) has a total of 5814 instances and consists of three  
301 modalities, local self-similarity features, SIFT features and SURF features, and contains 10  
302 clusters. Scene-15 <sup>[29]</sup> has 3000 instances and consists of three modalities consisting of LBP  
303 features, GIST features and CENTRIST features containing 15 clusters. CUB  
304 (<http://www.vision.caltech.edu/visipedia/CUB-200-2011.html>) contains 50 clusters totaling 2889  
305 data instances. Two modalities consist of 1024-dimensional image features extracted by  
306 GoogleNet and 1024-dimensional corresponding text features <sup>[30]</sup>.  
307 flowers(<http://www.robots.ox.ac.uk/~vgg/data/flowers/102/>) contains 50 clusters totaling 3235  
308 data instances. The two modalities consist of GoogleNet extracted 1024-dimensional image  
309 features and 1024-dimensional corresponding text features. Both image features are removed at  
310 the time of input. The specific information of the adopted dataset is shown in Table 1:

311

Table 1 The specification of the Dataset

312

### 313 4.2 Experiment details

314 After completing the data collection of the dataset, it is necessary to determine the relevant  
315 details of the paper, mainly including: model evaluation indexes, model training process and so  
316 on. In order to evaluate the experimental results, we adopt three evaluation indexes: Accuracy  
317 (ACC), Normalized Mutual Information (NMI) and Adjusted Rand Index (ARI), all of which are  
318 higher to indicate better performance. ARI), all of which are higher for better performance.  
319 Clustering accuracy Used to compare the clustering assignment labels with the true labels  
320 provided by the data.

321

$$ACC = \frac{\sum_{i=1}^N \delta(s_i, \text{map}(c_i))}{N} \quad (11)$$

322

where  $s_i$  denotes the true label of the first  $i$  true label of the first sample, and  $c_i$  denotes the

323 label assigned by the clustering algorithm to the  $i$  the label assigned to the first sample by the  
 324 clustering algorithm, and  $N$  is the total number of data, and  $\text{map}^{\text{argmax}}(c_i)$  Calculate  $c_i$  to  $s_i$  The  
 325 mapping between  $\delta$  is determined by the following formula:

$$326 \quad \delta(x,y) = \begin{cases} 1 & \text{if } x = y \\ 0 & \text{otherwise} \end{cases} \quad (12)$$

327 NMI is defined as the following equation.

$$328 \quad NMI = \frac{MI(S,C)}{\max(H(S),H(C))} \quad (13)$$

329 where  $S, C$  are two different labels of the same sample, i.e., the true label and the cluster  
 330 assignment label, and  $MI(C, C')$  The NMI results do not change depending on the arrangement of  
 331 the clusters, and they are normalized to the cluster assignment labels.  $H(\cdot)$  The results of NMI  
 332 do not change depending on the arrangement of the clusters, they are normalized to the range of  
 333 0 for uncorrelated and 1 for perfectly correlated.  $[0, 1]$  The results of NMI do not change according  
 334 to the arrangement of clusters, and they are normalized to the range of 0 for no correlation and 1  
 335 for perfect correlation.

336 RI (Rand Index) represents the rate of correct decision making and is defined as.

$$337 \quad RI = \frac{TP + TN}{TP + TN + FP + FN} \quad (14)$$

338 where TP is true positive, TN is true negative, FP is the false positive and FN is the false  
 339 negative. The Rand index has values between  $[0, 1]$  The Rand Index (RI) has a value between 1  
 340 and 2, and the RI is 1 when the two classifications match.

341 Unsupervised Deep Embedding clustering (DEC) <sup>[31]</sup>, improved DEC (IDEC) <sup>[32]</sup> and Deep  
 342 Neural Networks for Spectral Clustering (SpectralNet) <sup>[33]</sup>, Deep canonically correlated auto-  
 343 encoders (DCCAE) <sup>[34]</sup> used for clustering analysis in clustering research are the more widely  
 344 used methods that are more mature and represent their respective fields. methods, so this paper  
 345 chooses the above methods for the comparison. After confirming the dataset and related indexes,  
 346 we trained the model, and the training methods used for different models are similar, and the  
 347 specific steps are shown in Algorithm1:

#### Algorithm 1: Training process of ATT-VAE for clustering

**Input:** AWA dataset, Scene dataset, CUB dataset, Flower dataset

##### Initialization.

Define the ATT-VAE.

Define the hyperparameters and Initialization.

Define the loss function.

Define the optimizer: Adam optimizer.

Define the number of training epochs.

**Feature extraction.**

Using the original features in the dataset

**Pre-training:** Initialize the pre-training step counter.

**while** pre-training step counter < pre-training steps do

    Sample a batch of data.

    Feed data to the ATT-VAE framework.

    Update model.

    Counter++;

**End**

**Parameters tuning**

Tuning counter definition TT.

**while** TT < Preset iteration **do**

    Feed sample data to the proposed network.

    Loss and gradients calculation.

    Model updated.

    Compute ACC, NMI and RI

    Save the optimal model

**end**

**Output:** Trained ATT-VAE

348 After completing the model building and training of the relevant data, we performed statistics for  
349 the model.

350

### 351 4.3 Experiment Result and Analysis

352 Based on the pertinent metrics and model training procedures elucidated in sections 4.1 and  
353 4.2, we subjected the data to diverse test sets and shall now elucidate the detailed clustering  
354 outcomes for each dataset. Table 2 and Figure 5 encapsulate the clustering results for the AWA  
355 dataset. Notably, the introduction of the deep network has manifestly enhanced clustering  
356 performance, with the proposed method showcased in this study surpassing conventional  
357 approaches in the present stage across all three metric categories: ACC, NMI, and RI. Indeed,  
358 the proposed method outperforms common techniques across all three metric types at this  
359 juncture.

360 Table 2 The comparison result of three indicators concerning AWA datasets

361

362 Figure 5 The comparison result of three indicators concerning AWA datasets

363

364 After completing the analysis of the AWA data, we similarly analyzed the data on the three

365 datasets SCENE, CUB, and Flower, the results of which are shown in figure 6,7,8, and the  
366 corresponding data results are given accordingly in Table 3,4,5.

367 Table 3 The comparison result of three indicators concerning SCECE datasets

368

369 Figure 6 The comparison result of three indicators concerning SCECE datasets

370

371 Table 4 The comparison result of three indicators concerning CUB datasets

372

373 Figure 7 The comparison result of three indicators concerning CUB datasets

374

375 Table 5 The comparison result of three indicators concerning Flower datasets

376

377 Figure 8 The comparison result of three indicators concerning Flower datasets

378

379 After completing the comparison of multiple methods, this paper also carries out batch size  
380 comparison experiments of the proposed method under different datasets, which are tested  
381 through eight batch sizes ranging from 2 to 128, and the corresponding boxplots obtained are  
382 shown in Figure 9:

383 Figure 9 The ACC for the different datasets using different batch sizes

384

385 In Figure 9, it's evident that the variance in clustering results across different batch sizes is  
386 relatively modest. This observation underscores the inherent robustness of the method advanced  
387 in this paper.

388 Examining the data presented in the icon, it becomes evident that the ATT-VAE model, as  
389 introduced in this paper, boasts commendable generalization prowess and data clustering  
390 acumen. This is particularly conspicuous in the case of the CUB and Flower datasets, which  
391 feature fewer attributes and categories. In such scenarios, the clustering efficacy is notably  
392 pronounced. This attribute bodes well for the application of this method in the financial analysis  
393 of low-dimensional data characteristic of financial system analysis. As an extension of this  
394 approach, the paper now extends its ambit to the realm of economic and financial research  
395 (<https://cn.gtadata.com/>). Leveraging solvency, operational capacity, and profitability indicators  
396 as provided by this source, the model undertakes risk analysis through clustering, stratifying  
397 entities into high-risk and low-risk categories. This dataset is denoted as the Finance database.  
398 The results pertaining to ACC and NMI under this database are depicted in Figure 10.

399 Figure 10 The ACC and NMI result with the Finance datasets

400

401 Figure 10 illustrates a discernible trend: as the complexity of the deep network progressively  
402 intensifies, the clustering accuracy of the model registers a corresponding increase. Notably, the  
403 method proposed in this paper exhibits a notable advantage in terms of accuracy.

## 404 **5 Discussion and Conclusion**

405 In this study, we have introduced an innovative deep clustering paradigm utilizing ATT-  
406 VAE, with the objective of facilitating the adaptive clustering of financial perils within the realm of  
407 financial data. The model's performance has been exhaustively assessed employing common  
408 high-dimensional, low-dimensional clustering public datasets, along with real-world financial risk  
409 data distinguished by practical relevance. The experimental findings presented herein  
410 substantiate the effectiveness of the approach delineated in this manuscript. By harnessing  
411 diverse clustering methodologies and enhancing the VAE model through the integration of  
412 attention mechanisms, our method achieves significantly enhanced clustering outcomes. The  
413 approach has further demonstrated its prowess in authentic financial data assessments,  
414 boasting a clustering accuracy surpassing 70%. This accomplishment provides robust validation  
415 for future undertakings in financial analysis and data management

416 Anticipating forthcoming work, we envision broadening the adaptability of the model to  
417 embrace a plethora of financial data formats while refining its data processing capabilities.  
418 Furthermore, we intend to delve into advanced optimizations for the clustering network and the  
419 augmentation of model capabilities through the incorporation of techniques such as  
420 reinforcement learning. Although the VAE model employed in this investigation exhibits robust  
421 clustering capabilities, we will explore avenues to render the model more streamlined in the  
422 future. Furthermore, for financial data characterized by judiciously selected and processed  
423 features, the data analysis may potentially be carried out by a more lightweight clustering  
424 model. Thus, the extraction of features from the model proposed in this paper, as well as from  
425 related deep clustering models, constitutes a central focus for future research, with the objective  
426 of attaining more comprehensive features.=.

## 427 **Data Availability**

428 The dataset employed in this investigation is made readily available and accessible to interested  
429 parties.

430

## 431 **Conflicts of Interest**

432 The author declares that there are no conflicts of interest.

433

## 434 Funding Statement

435 This work received no fundings.

## 436 Acknowledgments

I would like to thank the anonymous reviewers whose comments and suggestions helped improve this manuscript.

437

## 438 Reference

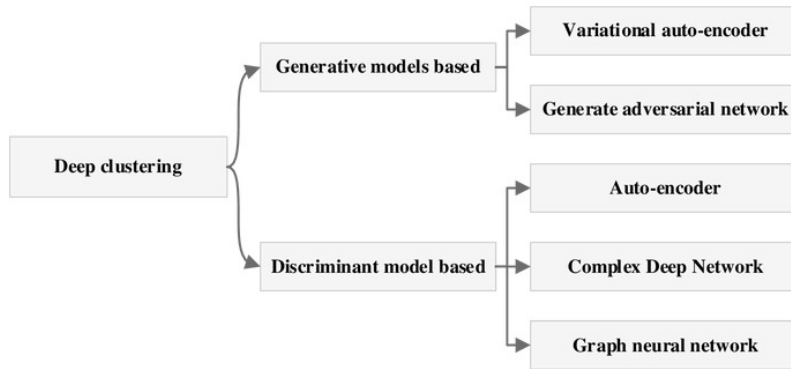
- 439 [1] Loughran T, McDonald B. Textual analysis in accounting and finance: A survey[J]. Journal of  
440 Accounting Research, 2016, 54(4): 1187-1230.
- 441 [2] Goodell J W, Kumar S, Lim W M. Artificial intelligence and machine learning in finance:  
442 Identifying foundations, themes, and research clusters from bibliometric analysis[J]. Journal  
443 of Behavioral and Experimental Finance, 2021, 32: 100577.
- 444 [3] Goodell J W, Kumar S, Lim W M. Artificial intelligence and machine learning in finance:  
445 Identifying foundations, themes, and research clusters from bibliometric analysis[J]. Journal  
446 of Behavioral and Experimental Finance, 2021, 32: 100577.
- 447 [4] Karim M R, Beyan O, Zappa A. Deep learning-based clustering approaches for  
448 bioinformatics[J]. Briefings in bioinformatics, 2021, 22(1): 393-415.
- 449 [5] Shi X, Wang Z, Zhao H. Threshold-free phase segmentation and zero velocity detection for  
450 gait analysis using foot-mounted inertial sensors[J]. IEEE Transactions on Human-Machine  
451 Systems, 2022, 53(1): 176-186.
- 452 [6] Lin W Y, Hu Y H, Tsai C F. Machine learning in financial crisis prediction: a survey[J]. IEEE  
453 Transactions on Systems, Man, and Cybernetics, Part C (Applications and Reviews), 2011,  
454 42(4): 421-436.
- 455 [7] Ohlson J. Financial Ratios And The Probabilistic Prediction Of Bankruptcy[J]. Journal of  
456 Accounting Research, 1980, 18(1): 109-131.
- 457 [8] Shin K S, Lee T S, Kim H J. An Application of Support Vector Machines in Bankruptcy  
458 Prediction Model[J]. Expert Systems with Applications, 2005, 28(1): 127-135.
- 459 [9] Atiya A F. Bankruptcy prediction for credit risk using neural networks: A survey and new  
460 results[J]. IEEE Transactions on Neural Networks, 2001, 12(4): 929-929.
- 461 [10] M. D. Odom, Sharda R. A neural network model for bankruptcy prediction[C]//Neural  
462 Networks, 1990. 1990 IJCNN International Joint Conference on. IEEE, 2012.
- 463 [11] Marcano-Cedeno A, Marin-De-La-Barcelona A, Jiménez-Trillo J, Pinuela J A, Andina D.  
464 Artificial metaplasticity neural network applied to credit scoring[J]. International journal of  
465 neural systems, 2011, 21(04): 311-317.
- 466 [12] Hosaka T. Bankruptcy prediction using imaged financial ratios and convolutional neural  
467 networks[J]. Expert systems with applications, 2019, 117: 287-299.

- 468 [13] Ahmed M, Seraj R, Islam S M S. The k-means algorithm: A comprehensive survey and  
469 performance evaluation[J]. *Electronics*, 2020, 9(8): 1295.
- 470 [14] Patnaik A K, Bhuyan P K, Rao K V K. Divisive Analysis (DIANA) of hierarchical clustering and  
471 GPS data for level of service criteria of urban streets[J]. *Alexandria Engineering Journal*,  
472 2016, 55(1): 407-418.
- 473 [15] Guha S, Rastogi R, Shim K. Cure: An efficient clustering algorithm for large databases[J]. *ACM*  
474 *Sigmod record*, 1998, 27(2): 73-84.
- 475 [16] Nayak J, Naik B, Behera H S. Fuzzy C-means (FCM) clustering algorithm: a decade review  
476 from 2000 to 2014[C]// *Computational Intelligence in Data Mining-Volume 2: Proceedings of*  
477 *the International Conference on CIDM, 20-21 December 2014*. Springer India, 2015: 133-  
478 149.
- 479 [17] Krinidis S, Chatzis V. A robust fuzzy local information C-means clustering algorithm[J]. *IEEE*  
480 *transactions on image processing*, 2010, 19(5): 1328-1337.
- 481 [18] Seal A, Karlekar A, Krejcar O. Fuzzy c-means clustering using Jeffreys-divergence based  
482 similarity measure[J]. *Applied Soft Computing*, 2020, 88: 106016.
- 483 [19] Wang X, Qian B, Davidson I. On constrained spectral clustering and its applications[J]. *Data*  
484 *Mining and knowledge discovery*, 2014, 28: 1-30.
- 485 [20] Chen W Y, Song Y, Bai H. Parallel spectral clustering in distributed systems[J]. *IEEE*  
486 *transactions on pattern analysis and machine intelligence*, 2010, 33(3): 568-586.
- 487 [21] Song C, Liu F, Huang Y. Auto-encoder based data clustering[C]// *Progress in Pattern*  
488 *Recognition, Image Analysis, Computer Vision, and Applications: 18th Iberoamerican*  
489 *Congress, CIARP 2013, Havana, Cuba, November 20-23, 2013, Proceedings, Part I 18*.  
490 Springer Berlin Heidelberg, 2013: 117-124.
- 491 [22] Xie J, Girshick R, Farhadi A. Unsupervised deep embedding for clustering  
492 analysis[C]// *International conference on machine learning*. PMLR, 2016: 478-487.
- 493 [23] Yang B, Fu X, Sidiropoulos N D. Towards k-means-friendly spaces: Simultaneous deep  
494 learning and clustering[C]// *international conference on machine learning*. PMLR, 2017: 3861-  
495 3870.
- 496 [24] Min E, Guo X, Liu Q. A survey of clustering with deep learning: From the perspective of  
497 network architecture[J]. *IEEE Access*, 2018, 6: 39501-39514.
- 498 [25] Santhosh K K, Dogra D P, Roy P P. Vehicular trajectory classification and traffic anomaly  
499 detection in videos using a hybrid CNN-VAE Architecture[J]. *IEEE Transactions on Intelligent*  
500 *Transportation Systems*, 2021, 23(8): 11891-11902.
- 501 [26] Xu C, Zhang Y, Chen H, Dong L, Wang W. A fairness-aware graph contrastive learning  
502 recommender framework for social tagging systems, *Information Sciences*, 640, 119064,  
503 2023.
- 504 [27] Krizhevsky A, Sutskever I, Hinton G E. Imagenet classification with deep convolutional neural  
505 networks[J]. *Advances in neural information processing systems*, 2012, 25.
- 506 [28] Targ S, Almeida D, Lyman K. Resnet in resnet: Generalizing residual architectures[J]. *arXiv*  
507 *preprint arXiv:1603.08029*, 2016.
- 508 [29] Fei-Fei L, Perona P. A bayesian hierarchical model for learning natural scene

- 509 categories[C]//2005 IEEE Computer Society Conference on Computer Vision and Pattern  
510 Recognition (CVPR'05). IEEE, 2005, 2: 524-531.
- 511 [30] Reed S, Akata Z, Lee H. Learning deep representations of fine-grained visual  
512 descriptions[C]//Proceedings of the IEEE conference on computer vision and pattern  
513 recognition. 2016: 49-58.
- 514 [31] Xie J, Girshick R, Farhadi A. Unsupervised deep embedding for clustering  
515 analysis[C]//International conference on machine learning. PMLR, 2016: 478-487.
- 516 [32] Guo X, Gao L, Liu X. Improved deep embedded clustering with local structure  
517 preservation[C]// International Joint Conferences on Artificial Intelligence. 2017: 1753-1759.
- 518 [33] Shaham U, Stanton K, Li H. Spectralnet: Spectral clustering using deep neural networks[J].  
519 arXiv preprint arXiv:1801.01587, 2018.
- 520 [34] Wang W, Arora R, Livescu K. On deep multi-view representation learning[C]//International  
521 conference on machine learning. PMLR, 2015: 1083-1092.  
522

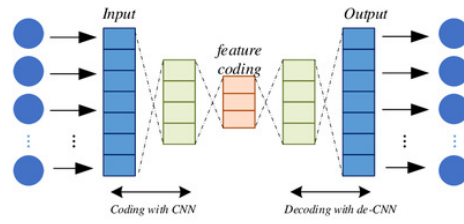
# Figure 1

Figure 1 The deep clustering methods



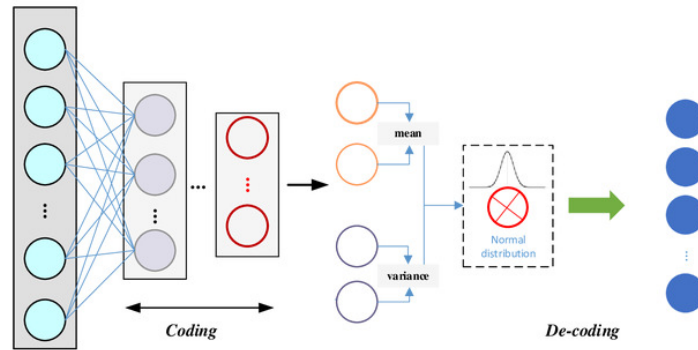
## Figure 2

Figure 2 Structure of self-encoder



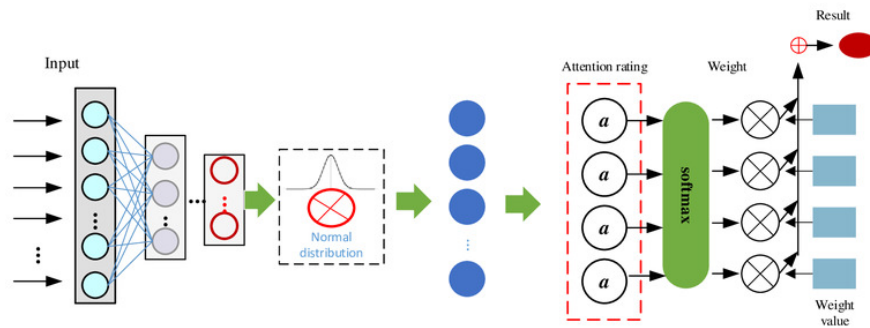
## Figure 3

Figure 3 The framework for the VAE



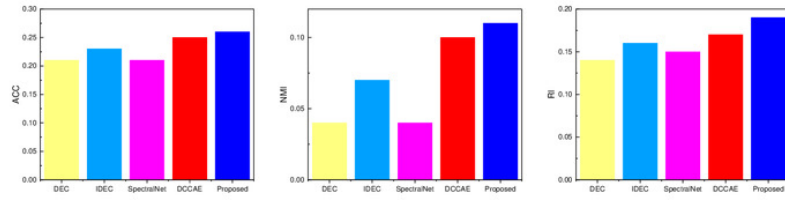
## Figure 4

Figure 4 Framework of the proposed ATT-VAE



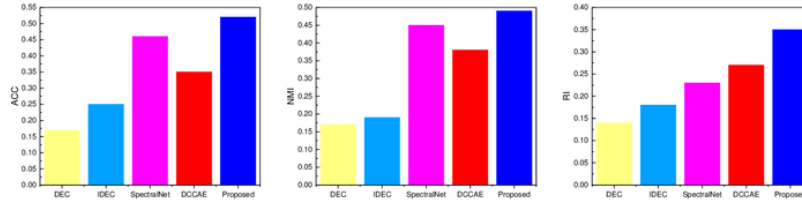
## Figure 5

Figure 5 The comparison result of three indicators concerning AWA datasets



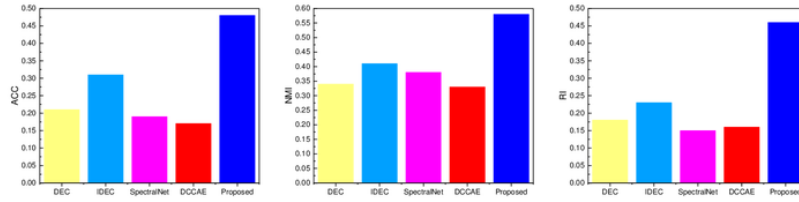
## Figure 6

Figure 6 The comparison result of three indicators concerning SCECE datasets



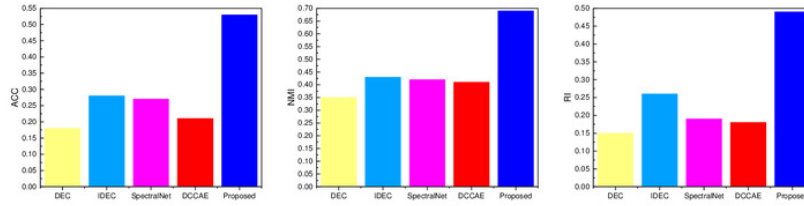
## Figure 7

Figure 7 The comparison result of three indicators concerning CUB datasets



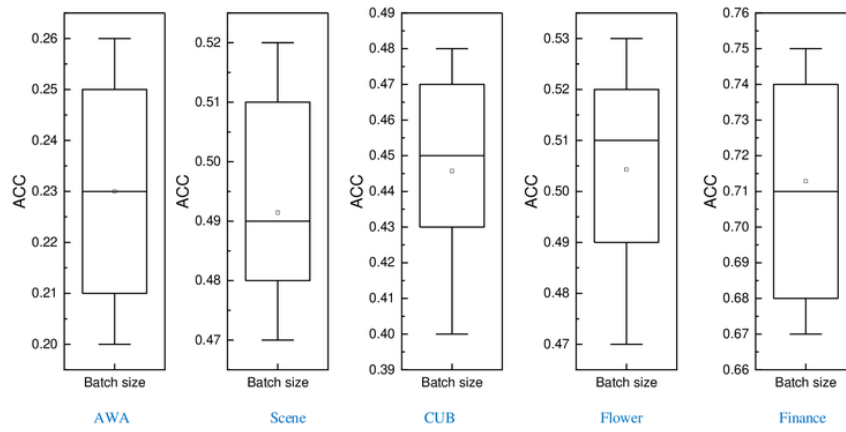
## Figure 8

Figure 8 The comparison result of three indicators concerning Flower datasets



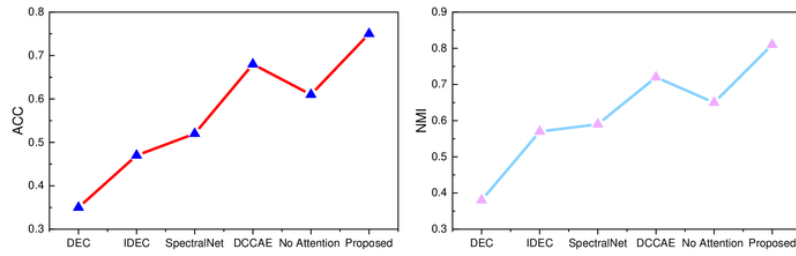
## Figure 9

Figure 9 The ACC for the different datasets using different batch sizes



## Figure 10

Figure 10 The ACC and NMI result with the Finance datasets



**Table 1** (on next page)

Table 1 The specification of the Dataset

Dataset	Modal	Samples	Cluster
AwA	3	5814	10
Scene	3	3000	3
CUB	2	2889	2
Flower	2	3235	2

1

**Table 2** (on next page)

Table 2 The comparison result of three indicators concerning AWA datasets

	DEC	IDEC	SpectralNet	DCCAE	Proposed
ACC	0.21	0.23	0.21	0.25	0.26
NMI	0.04	0.07	0.04	0.1	0.11
RI	0.14	0.16	0.15	0.17	0.19

1

**Table 3** (on next page)

Table 2 The comparison result of three indicators concerning AWA datasets

	DEC	IDEC	SpectralNet	DCCAIE	Proposed
ACC	0.17	0.25	0.46	0.35	0.52
NMI	0.17	0.19	0.45	0.38	0.49
RI	0.14	0.18	0.23	0.27	0.35

1

**Table 4** (on next page)

Table 4 The comparison result of three indicators concerning CUB datasets

	DEC	IDEC	SpectralNet	DCCAE	Proposed
ACC	0.21	0.31	0.19	0.17	0.48
NMI	0.34	0.41	0.38	0.33	0.58
RI	0.18	0.23	0.15	0.16	0.46

1

**Table 5** (on next page)

Table 5 The comparison result of three indicators concerning Flower datasets

	DEC	IDEC	SpectralNet	DCCAIE	Proposed
ACC	0.18	0.28	0.27	0.21	0.53
NMI	0.35	0.43	0.42	0.41	0.69
RI	0.15	0.26	0.19	0.18	0.49

1